Report No. DOE/ER/06042-3

Contract No.
DE-AS05-78ER06042

MASTER

CORRELATIONS OF PHYSICAL AND CHEMICAL PROPERTIES OF LANTHANIDE OXIDES WITH CATALYTIC BEHAVIORS

Progress Report for the Period
September 1, 1980 - August 31, 1981

by

Michael P. Rosynek

Department of Chemistry
Texas A & M University
College Station, Texas 77843

Submitted:
April, 1981

DISTRIBUTION OF THIS DOCUMENT IS UNLIMITED
MGW

I. RESEARCH SCOPE AND OBJECTIVES

The objective of our research is to investigate correlations that exist between the heterogeneous catalytic behaviors of lanthanide oxides for certain test reactions and corresponding periodic trends in the physical/chemical parameters of these materials. Particular emphasis has been placed on identifying and characterizing the effects of magnetic and electronic properties, imparted by varying cationic 4f-electron configurations, as well as solid-state phase transitions and surface basicities on both the activity/selectivity behaviors that are exhibited by selected members of this oxide series and on the chemical/structural natures of their catalytic sites.

II. DESCRIPTION OF RESEARCH EFFORT

The diagnostic test reaction utilized for this study has been the catalytic decomposition of gaseous ethanol, for which simultaneous dehydration to ethylene and dehydrogenation to acetaldehyde occur in varying ratios over all of the lanthanide oxides in the temperature range 300-400°C. This dual-pathway reaction was chosen because its two processes are likely to require separate types of catalytic surface sites having distinctly different chemical/structural natures. Because the surfaces of many metal oxides exhibit multiple - site features, the utility of this approach may be of general significance for oxide catalysts in addition to those of the rare earths, since it has allowed characterizations to be made of both the behaviors of individual kinds of surface sites as well as their various interactions and combined operation.

Using the batch reaction/analysis system that has been described in a previous Progress Report, we have completed separate characterizations of the behaviors of both La_2O_3 and Nd_2O_3 for ethanol decomposition, and have recently begun to investigate the corresponding properties of Pr_2O_3 for this reaction. Somewhat surprisingly, in view of their dissimilar cationic electronic/magnetic properties and differing surface basicities, the catalytic behaviors of La_2O_3 and Nd_2O_3 are virtually identical in all respects for both pathways of the alcohol conversion. This similarity involves not only their initial activity/selectivity parameters, but also their responses to variations in catalyst preparation/pretreatment conditions, crystallographic phase, and poisoning of the different kinds of catalytic sites. Moreover, our preliminary results for Pr_2O_3 indicate that its behavior also closely resembles those of La_2O_3 and Nd_2O_3. Because of this similarity, results obtained for the latter two oxides will be presented and discussed simultaneously for each of the alcohol decomposition pathways in the sections that follow.

1. Dehydration Pathway

With both La_2O_3 and Nd_2O_3, the dehydration pathway predominates initially over that of dehydrogenation throughout the reaction temperature range 300-400°C, accounting for 85-95% of all ethanol converted. The process is exclusively uni-, rather than bi-, molecular, and the ethylene produced is inert to secondary reactions, including saturation by the hydrogen produced during the dehydrogenation pathway. Initial dehydration rates, as determined by the rate of ethylene formations, over both oxides are unaffected by changes in surface hydroxyl concentration, but decrease monotonically with increasing catalyst pretreatment evacuation temperature in the range 400-1000°, as shown in Figs. 1 and 2, probably due to decreasing surface basicity brought about by increased anion ordering. The effect is qualitatively similar for both oxides, but is somewhat less pronounced with Nd_2O_3 than with La_2O_3. Additionally, both oxides undergo thermally-induced crystallographic phase transitions from

Figure 1   Effect of Catalyst Pretreatment Evacuation Temperature on Initial Rates of Ethanol Dehydration and Dehydrogenation over La_2O_3 at 350°C.

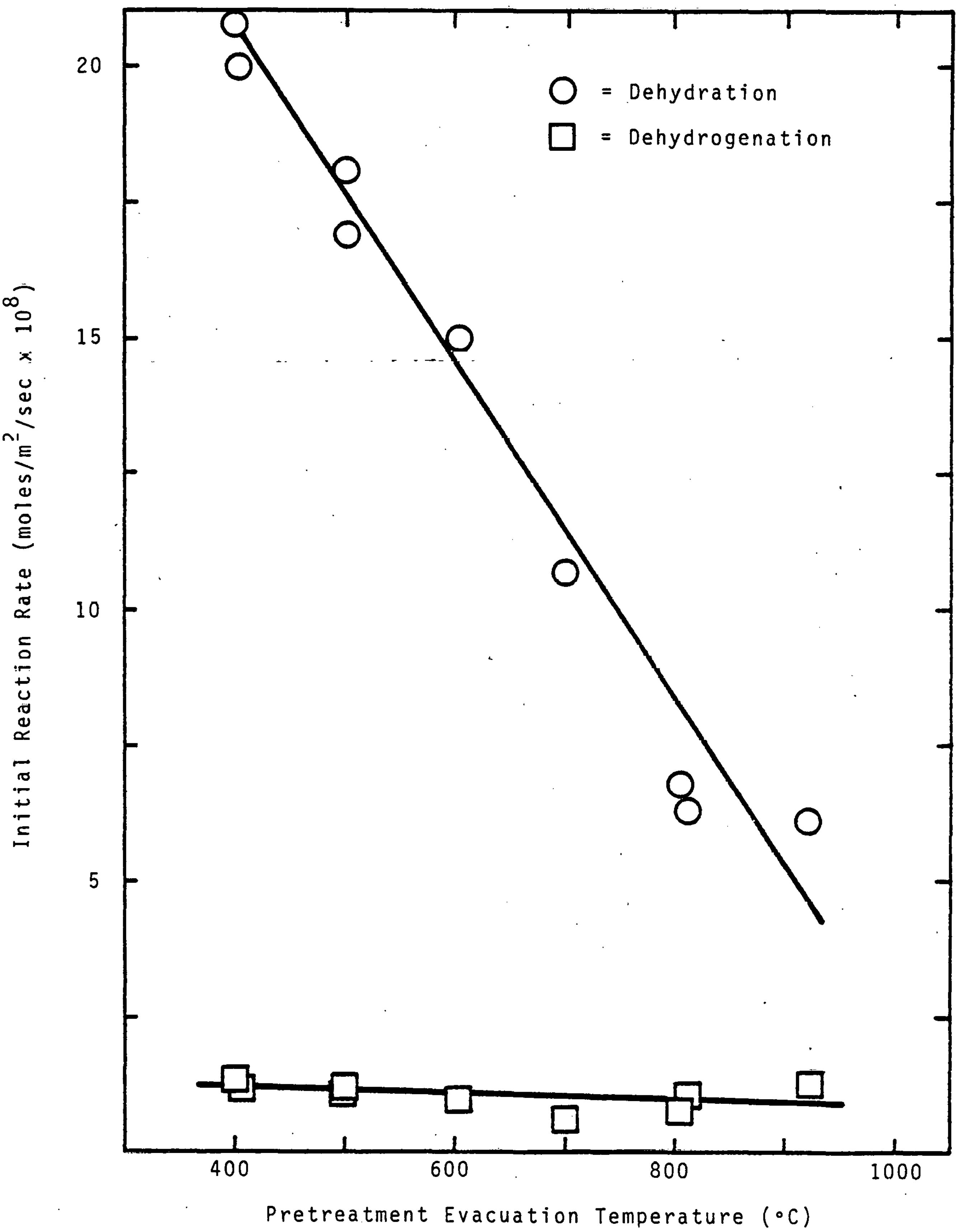
○ = Dehydration
□ = Dehydrogenation
Initial Reaction Rate (moles/m²/sec x 10⁸)
20
15
10
5
400
600
800
1000
Pretreatment Evacuation Temperature (°C)

Figure 2 Effect of Catalyst Pretreatment Evacuation Temperature on Initial Rates of Ethanol Dehydration and Dehydrogenation over Nd_2O_3 at 350°C.

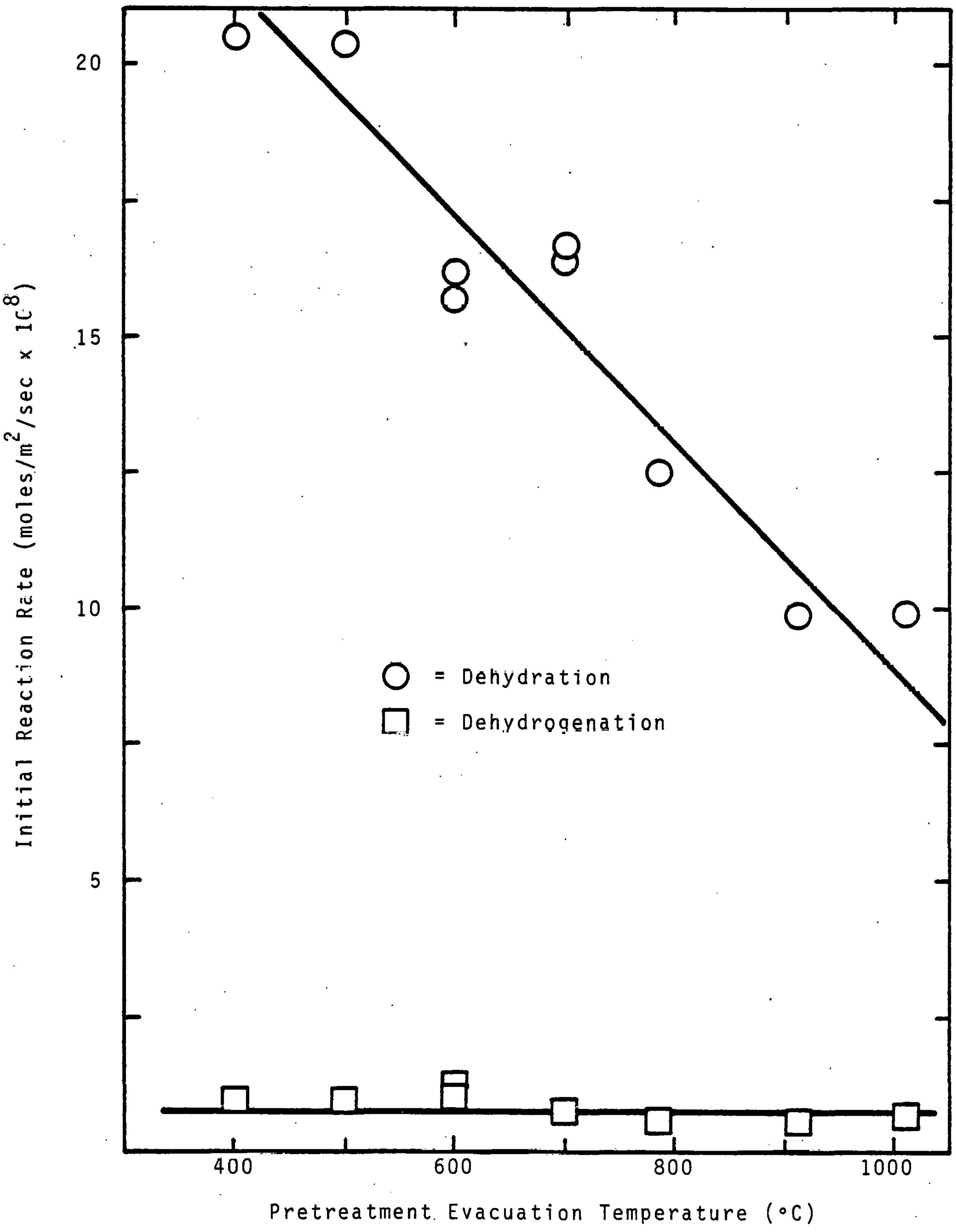

20
15
10
5
400
600
800
1000
Initial Reaction Rate (moles/m^2/sec x 10^8)
Pretreatment Evacuation Temperature (°C)
○ = Dehydration
□ = Dehydrogenation

the so-called C-type (body-centered cubic) structure to the A-type (hexagonal), as confirmed by x-ray diffraction measurements that are summarized in Figs. 3 and 4. In neither case, however, do the observed structural transformations directly correlate with changes in the rate of alcohol dehydration, which appears to be independent of oxide phase.

In individual experiments with both oxides, the initially high rate of dehydration invariably declines rapidly with increasing reaction time, the rate of decrease varying inversely with catalyst pretreatment temperature, as seen in Figs. 5 and 6 where selected data of this kind are presented. This decline in dehydration rate is attributed to an accumulation on the dehydration sites of acetate-like surface species that result from dissociative adsorption of acetaldehyde produced by the dehydrogenation pathway. Dynamic infrared spectroscopic studies employing both ethanol and acetaldehyde reactants have comfirmed that time-dependent decreases in the alcohol dehydration rate coincide closely with increasing surface acetate concentrations. This unusual secondary interaction of the two reaction pathways will be further discussed below in conjunction with the behavior of the dehydrogenation pathway.

The dehydration pathway on both La_2O_3 and Nd_2O_3 is also greatly suppresed by surface carbonate species that result from either pre-adsorption or co-reaction of carbon dioxide (Figs. 7 and 8), but is essentially unaffected by the Ln - CNO entities that poison the dehydrogenation process (vide infra). These results indicate that alcohol dehydration sites on both oxides involve basic surface O^{2-} ions that function (at least in the early stages of reaction) independently of the dehydrogenation sites.

Figure 3 Effect of Pretreatment Evacuation Temperature on Crystallographic Phase Composition of La_2O_3.

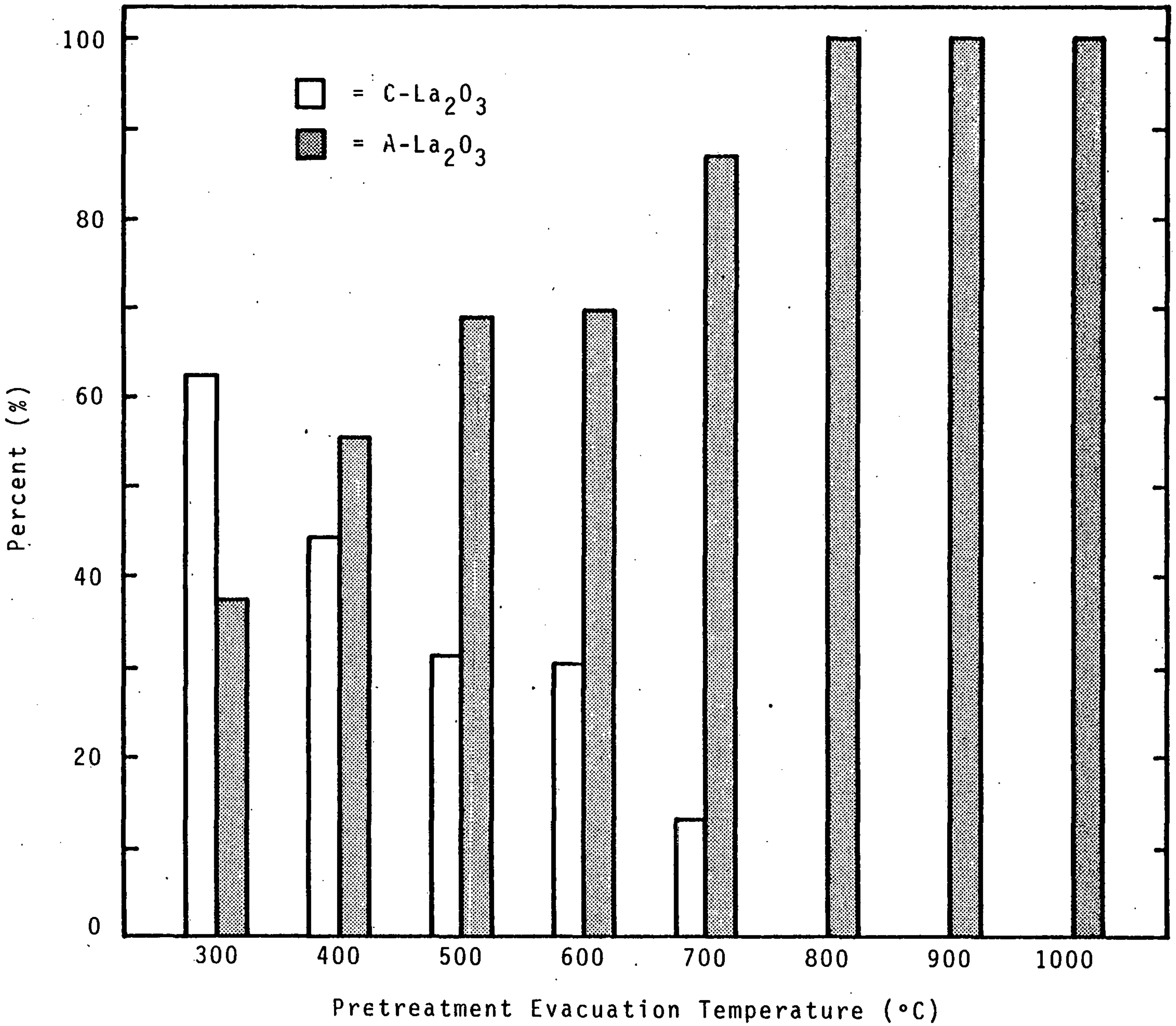

□ = C-La_2O_3
▨ = A-La_2O_3
100
80
60
40
20
0
Percent (%)
300
400
500
600
700
800
900
1000
Pretreatment Evacuation Temperature (°C)

<u>Figure 4</u> Effect of Pretreatment Evacuation Temperature on Crystallographic Phase Composition of Nd_2O_3.

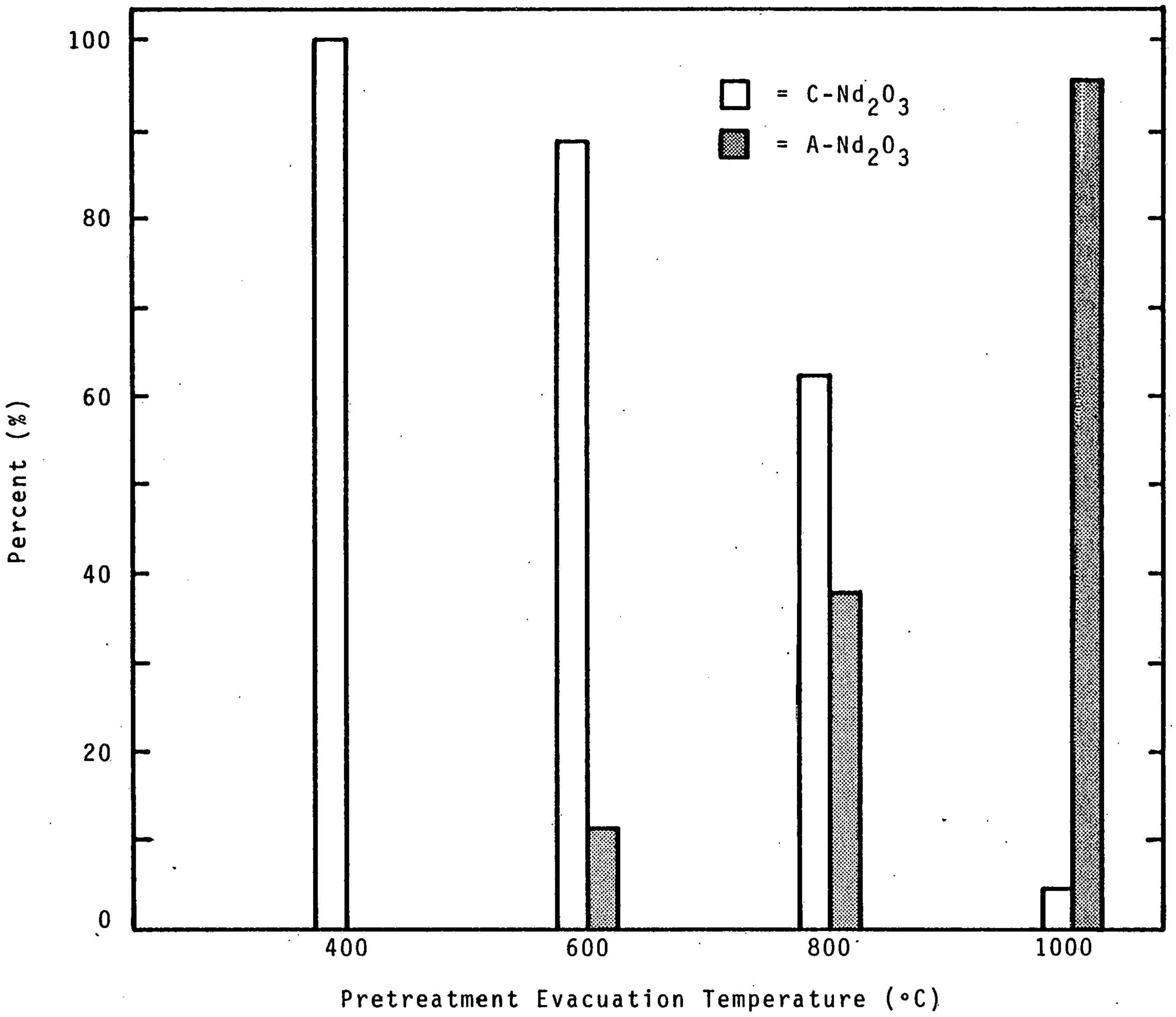
100
80
60
40
20
0
Percent (%)
□ = C-Nd_2O_3
▨ = A-Nd_2O_3
400
600
800
1000
Pretreatment Evacuation Temperature (°C)

Figure 5 Dependence of Ethanol Dehydration Rate on Reaction Time at 350°C over La_2O_3 Pretreated at the Indicated Temperatures.

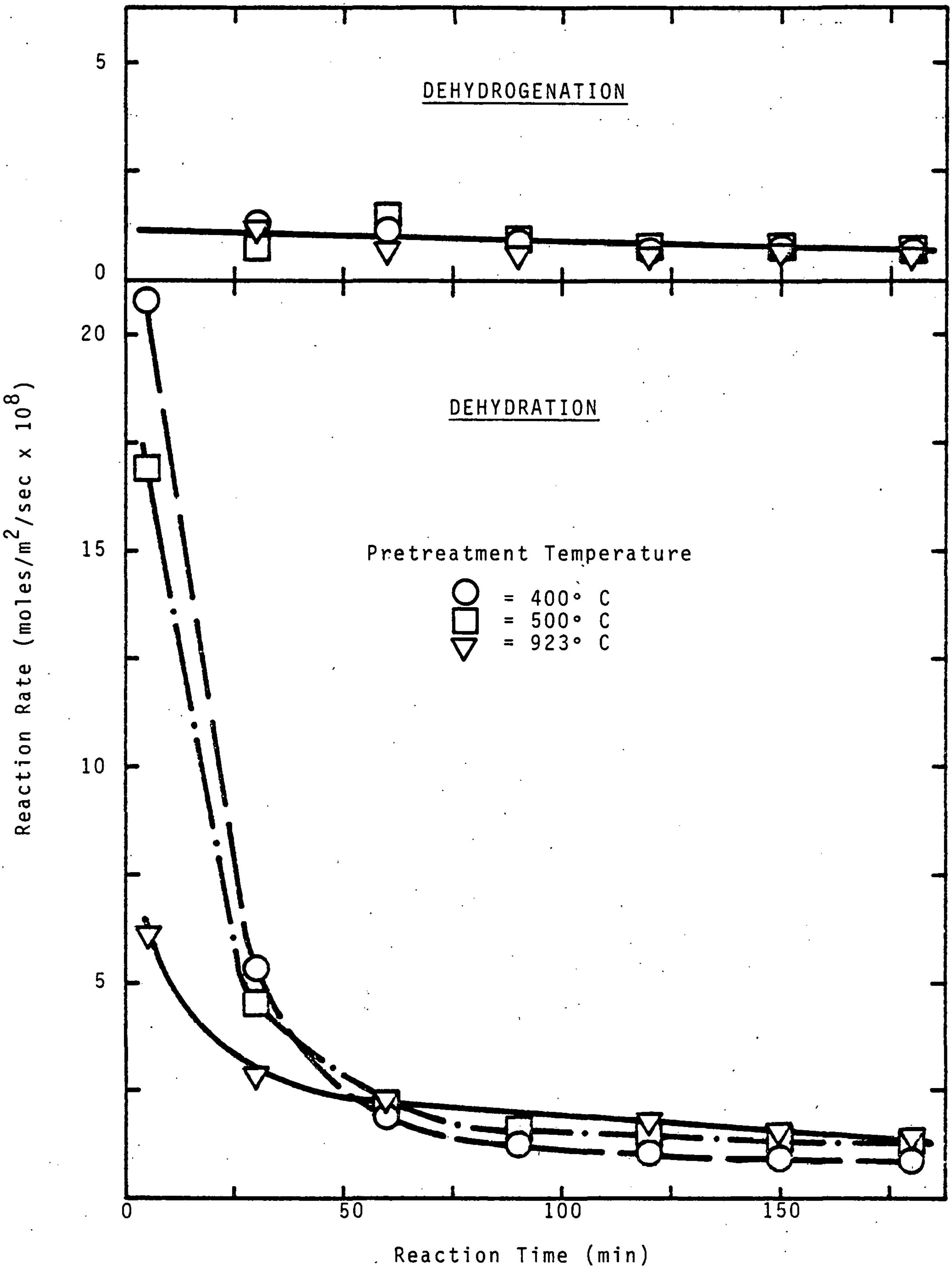
DEHYDROGENATION
DEHYDRATION
Pretreatment Temperature
○ = 400° C
□ = 500° C
▽ = 923° C
Reaction Rate (moles/m²/sec x 10⁸)
Reaction Time (min)
0
5
10
15
20
0
5
0
50
100
150

Figure 6 Dependence of Ethanol Dehydration Rate on Reaction Time at 350°C over Nd_2O_3 pretreated at the Indicated Temperatures.

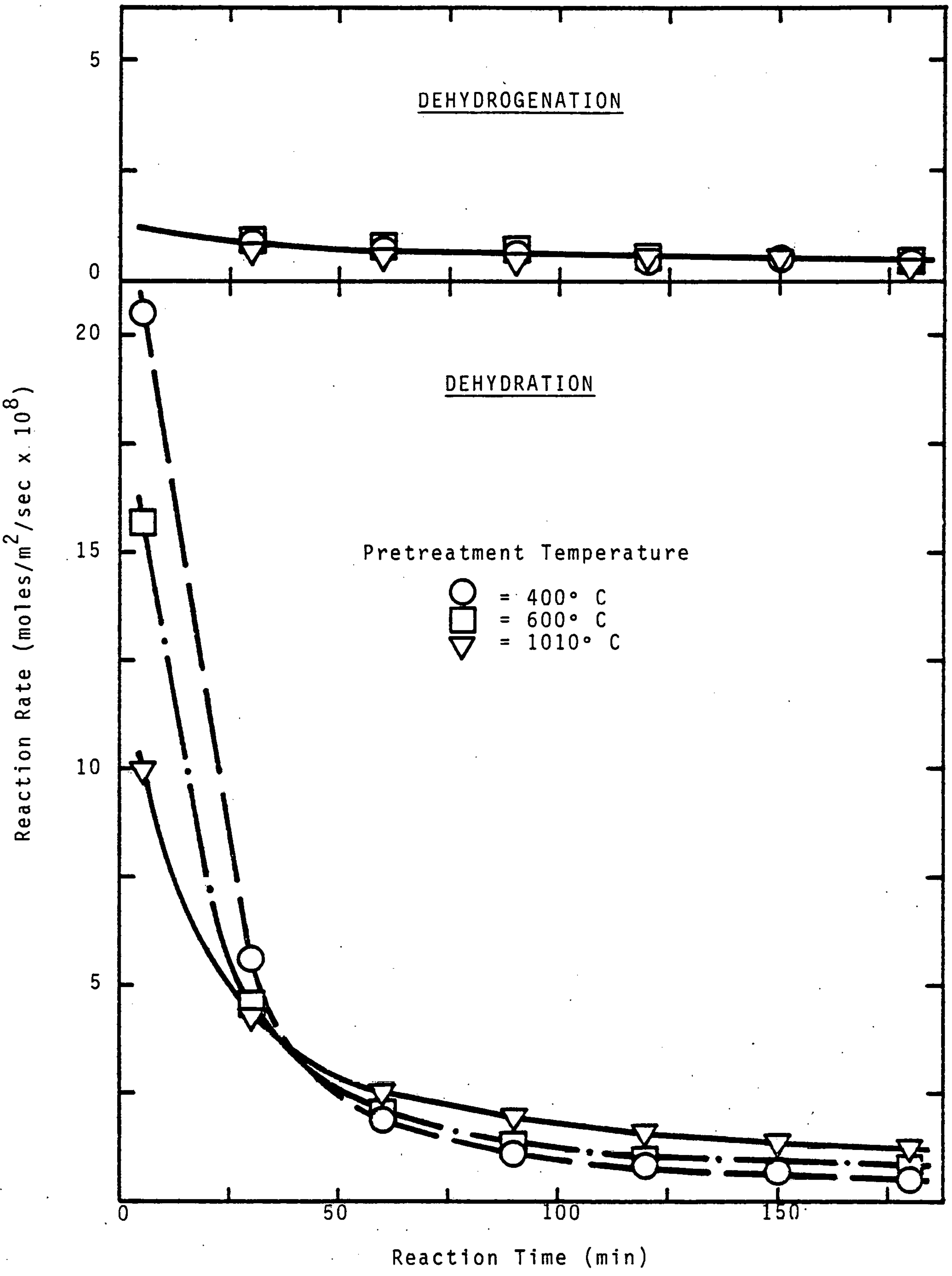
DEHYDROGENATION
DEHYDRATION
Pretreatment Temperature
○ = 400° C
□ = 600° C
▽ = 1010° C
Reaction Rate (moles/m^2/sec x 10^8)
Reaction Time (min)
0
5
0
5
10
15
20
0
50
100
150

Figure 7 Effect of Co-Reacted Carbon Dioxide on Ethanol Dehydration Rate at 350°C over La_2O_3 Pretreated at 400°C.

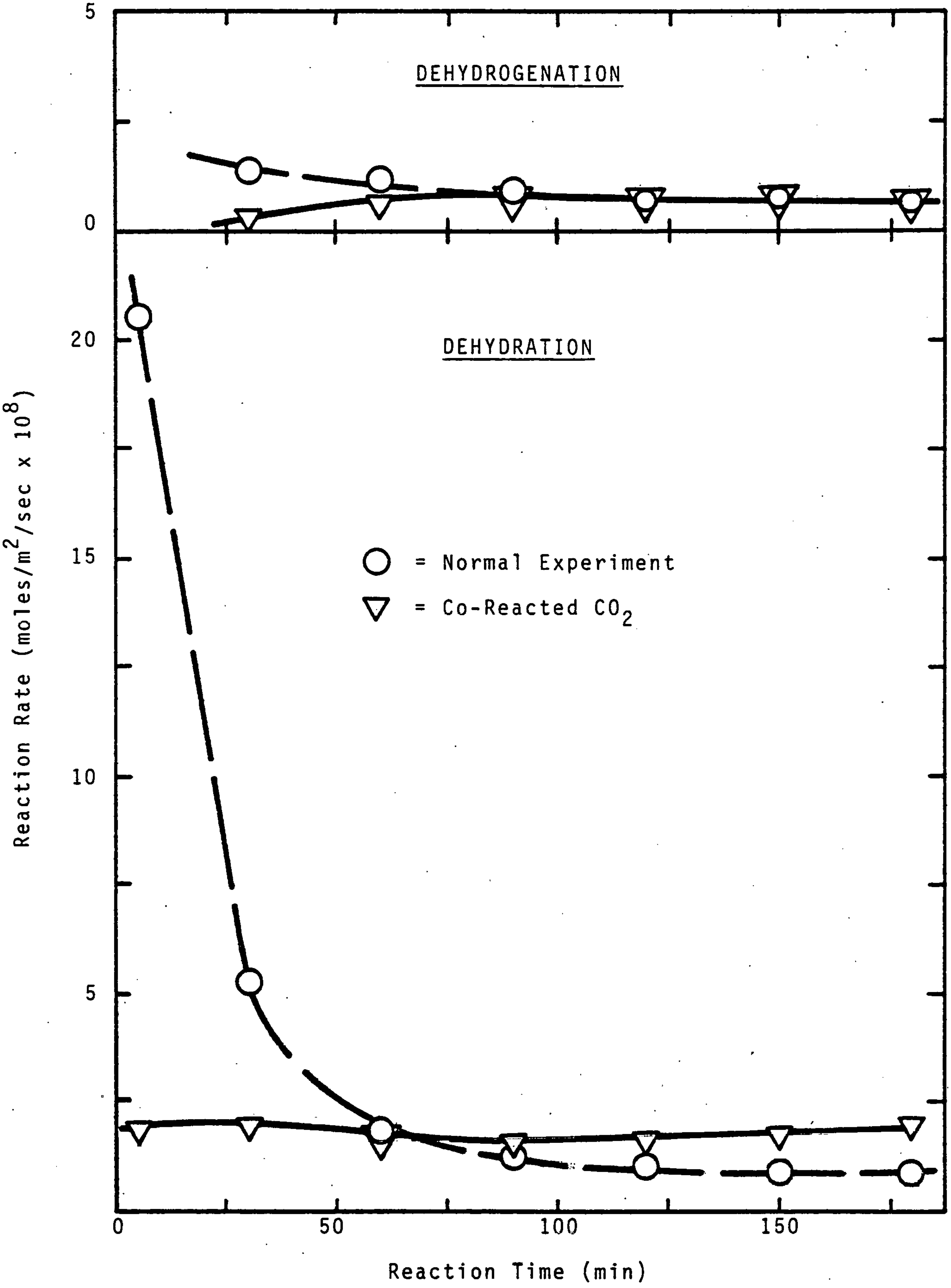
DEHYDROGENATION
DEHYDRATION
○ = Normal Experiment
▽ = Co-Reacted CO2
Reaction Rate (moles/m2/sec x 108)
Reaction Time (min)
5
0
20
15
10
5
0
50
100
150

Figure 8 Effect of Co-Reacted Carbon Dioxide on Ethanol Dehydration Rate at 350°C over Nd_2O_3 Pretreated at 400°C.

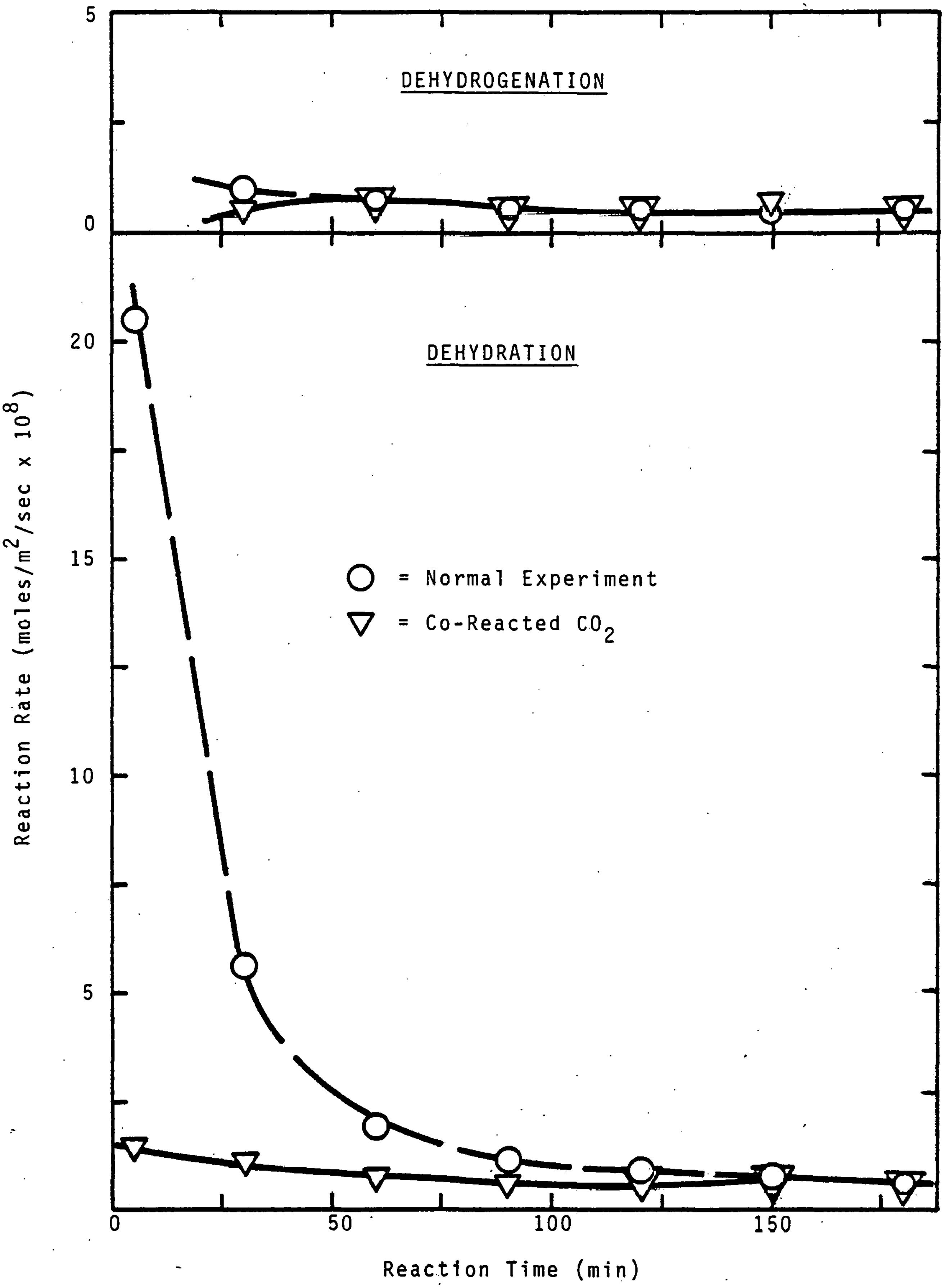
DEHYDROGENATION
DEHYDRATION
○ = Normal Experiment
▽ = Co-Reacted CO_2
Reaction Rate (moles/m^2/sec x 10^8)
Reaction Time (min)
5
0
20
15
10
5
0
50
100
150

2. Dehydrogenation Pathway

The alcohol dehydrogenation process shares certain empirical features with that of dehydration, viz., insensitivity to both surface hydroxyl concentration and crystallographic phase of the two oxide catalysts. However, in marked contrast to the behavior observed for the dehydration pathway, the rate of ethanol dehydrogenation, as determined by the initial rate of hydrogen formation, over both La_2O_3 and Nd_2O_3 is virtually unaffected by variations in catalyst pretreatment evacuation temperature in the range studied (Figs. 1 and 2), and does not decline appreciably with increasing reaction time during individual experiments, remaining almost constant up to at least 50% total conversion of alcohol reactant. These results provide further evidence for the dissimilar identities of the catalytic sites that are involved in the two pathways.

The rate of dehydrogenation over both oxides is unaffected by the presence of even a monolayer of the surface CO_3^{2-} species which effectively poison the O^{2-} dehydration sites, but is greatly suppressed, as shown in Figs. 9 and 10, by unidentate cyanate (-CNO) entities that result from prior exposure of either oxide to a mixture of CO_2 and NH_3 at 350°C. Infrared studies, utilizing various istotopically-labelled forms of CO_2 and NH_3, have confirmed both the identity of the cyanate moiety and, more importantly, the fact that it resides exclusively on Ln^{3+} sites on both oxides. Hence, alcohol dehydrogenation sites on La_2O_3 and Nd_2O_3 may be identified as requiring partially-exposed cationic centers which interact with reactant alcohol molecules independently of their simultaneous adsorption on O^{2-} sites. The apparent lack of sensitivity of either the number and/or intrinsic activity of such cationic sites to pretreatment temperature is as yet unclear.

Figure 9 Effect of Surface Cyanate Species on Ethanol Dehydrogenation Reaction at 350°C over La_2O_3 Pretreated at 800°C.

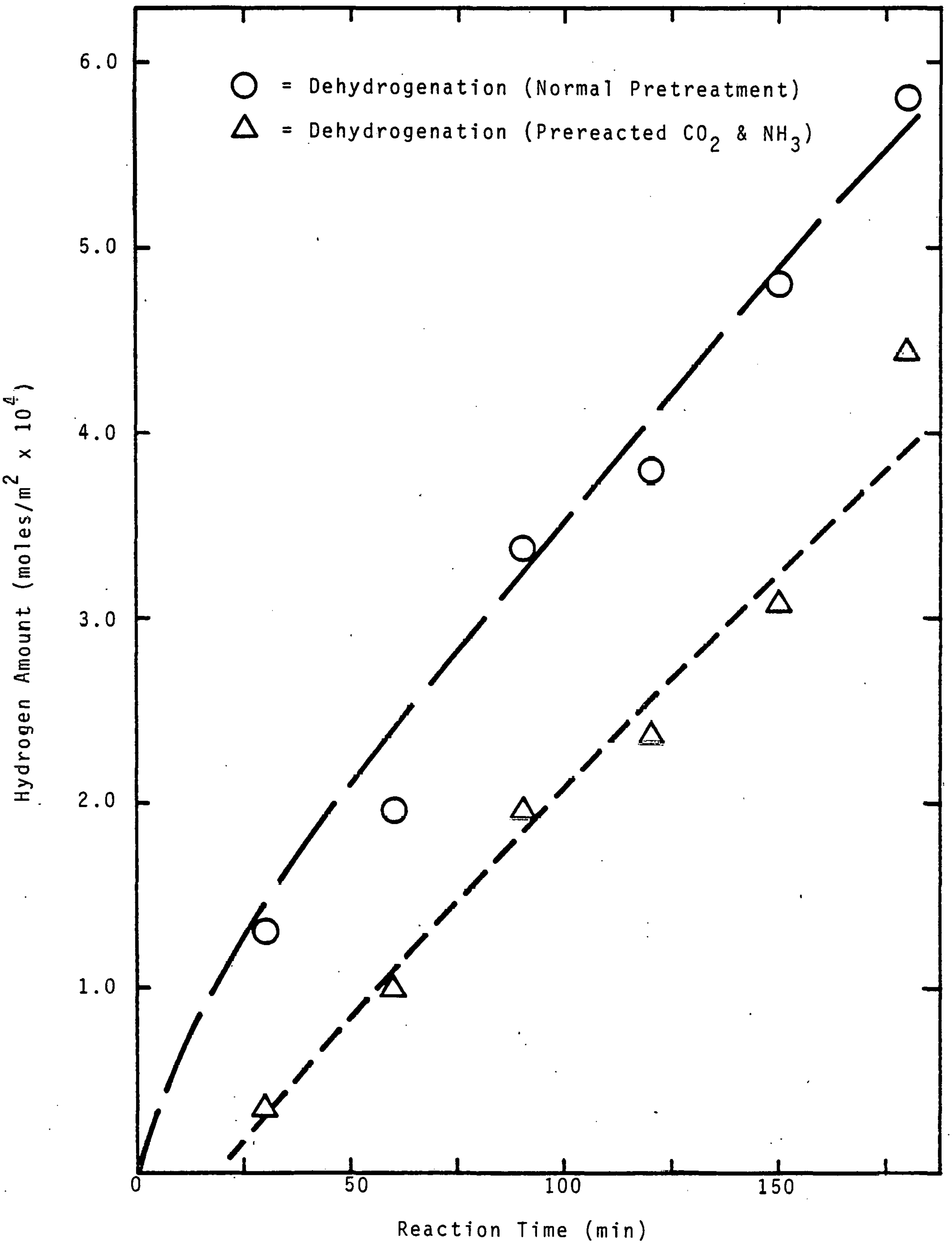
○ = Dehydrogenation (Normal Pretreatment)
△ = Dehydrogenation (Prereacted CO_2 & NH_3)
Hydrogen Amount (moles/m^2 x 10^4)
Reaction Time (min)
6.0
5.0
4.0
3.0
2.0
1.0
0
50
100
150

<u>Figure 10</u> Effect of Surface Cyanate Species on Ethanol Dehydrogenation Reaction at 350°C over Nd_2O_3 Pretreated at 800°C.

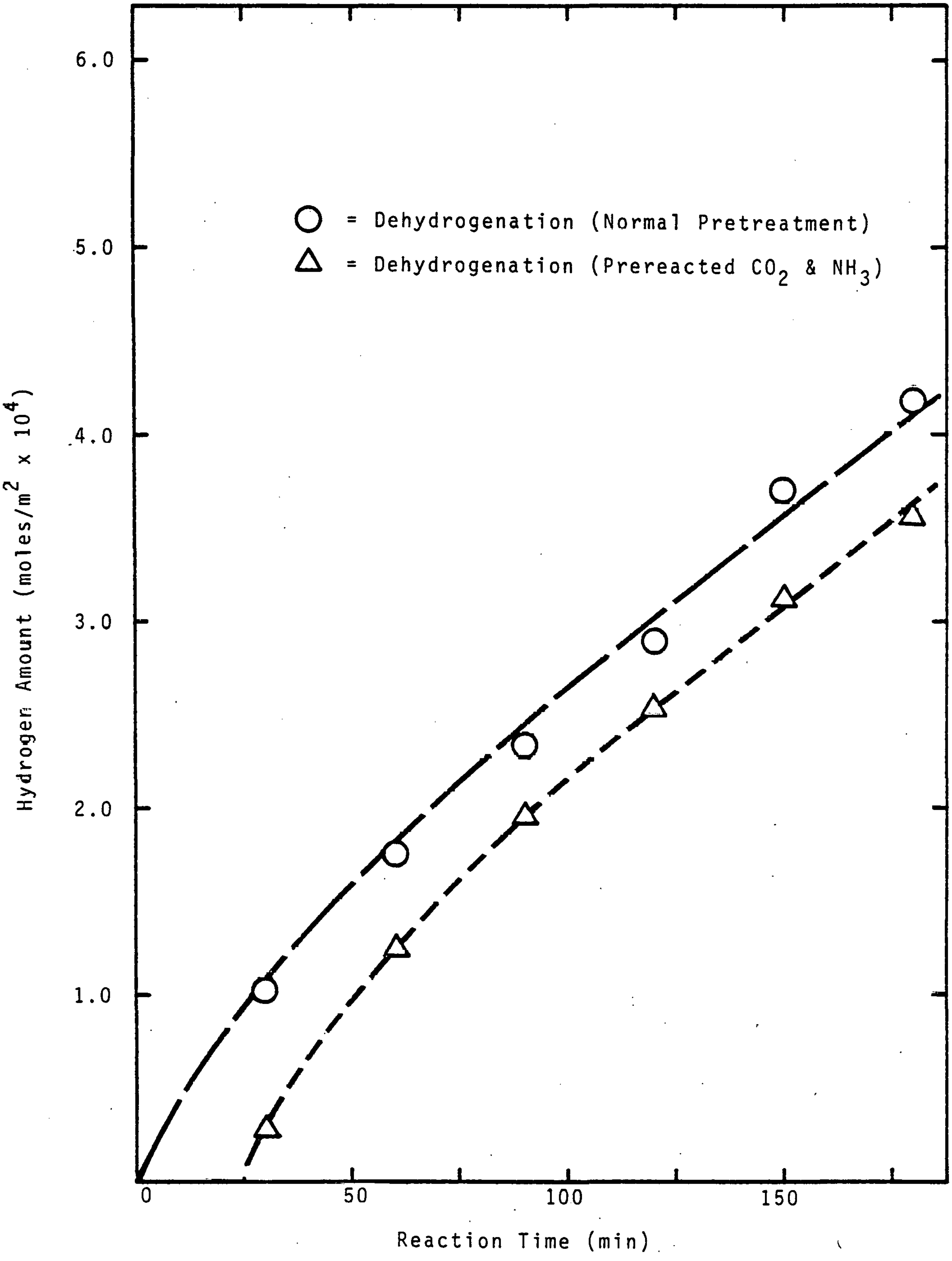
○ = Dehydrogenation (Normal Pretreatment)
△ = Dehydrogenation (Prereacted CO_2 & NH_3)
Hydrogen Amount (moles/m^2 x 10^4)
6.0
5.0
4.0
3.0
2.0
1.0
0
50
100
150
Reaction Time (min)

In comparison to the apparent mechanistic simplicity of the unimolecular dehydration pathway, the overall dehydrogenation process of ethanol over both oxide catalysts is more complex and not yet fully elucidated. Initial dehydrogenation of the alcohol in each case occurs on Ln^{3+} sites and generates acetaldehyde as the primary product. The latter quickly re-adsorbs dissociatively (via loss of the carbonyl H-atom) on O^{2-} dehydration sites to produce acetate-like surface species which undergo a series of secondary condensation-type reactions that lead to the formation of acetone, n-pentenes, CO_2, and additional H_2. In the case of La_2O_3, the presence of by-product water from the dehydration pathway enables the CO_2 thus produced to penetrate the oxide lattice to an extent of at least 5 to 6 monolayers, forming layer-like oxycarbonates. Such water-aided lattice penetration by CO_2 does not occur with Nd_2O_3 due to its smaller tervalent cation size, an observation that is in accord with the relatively greater ease of rehydration of La_2O_3 to the trihydroxide compared to that of Nd_2O_3.

Accumulation on O^{2-} sites of acetaldehyde-derived surface acetate species causes the previously-noted rapid declines in alcohol dehydration rates that are observed in individual experiments with both oxide catalysts. In addition to the infrared spectroscopic evidence discussed earlier, this conclusion is further supported by the fact that any experimental conditions that cause a decrease in initial alcohol dehydration rate (viz., increased catalyst pretreatment temperature or poisoning by surface CO_3^{2-}), while having a negligible effect on the initial rate of hydrogen formation, invariably suppress the extent of secondary condensation reactions and consequently result in increased amounts of gaseous acetaldehyde.

III. PRESENT RESEARCH

We are currently completing a more detailed characterization of the catalytic behavior of Pr_2O_3 for the ethanol decomposition process. Fragmentary results obtained thus far indicate that its properties for this reaction closely resemble those of La_2O_3 and Nd_2O_3. In view of the strong evidence supporting the participation of cationic sites these on oxides in the dehydrogenation pathway, we then plan to begin preliminary experiments utilizing certain of the various multi-valent oxides of Pr. These materials are characterized by varying, but well-defined, Pr^{3+}/Pr^{4+} cation ratios which we anticipate will strongly influence the activity/selectivity behavior of the alcohol decomposition reaction.